CHARACTERISTICS OF A BROAD-BAND WIDE-SCAN FRAGMENTED APERTURE PHASED ARRAY ANTENNA

Anders Ellgardt and Patrik Persson

Div. of Electromagnetic Engineering, Royal Institute of Technology, Teknikringen 33, 10044 Stockholm, Sweden, anders.ellgardt@ee.kth.se, patrik.persson@ee.kth.se

ABSTRACT

In this paper a phased array antenna is described that is designed with the help of a genetic algorithm for scan angles out to 60° from broadside. The focus is on simplifying the manufacturing of the diagonally adjoining pixels and on numerical results for thin antennas. The effects of the corner to corner contacts are studied and results for two synthesized elements are presented.

Key words: fragmented aperture, broad-band, phased array, wide-scan.

1. INTRODUCTION

Broad-band wide-scan planar phased arrays are suitable for multiple applications and are useful both in military and commercial sectors. For airborne applications the size of the antenna is important, and benefits with thin and light-weight antennas are evident. The size of the antenna aperture of the phased array is restricted by the desired directivity, so to further reduce weight and cost multi-role capabilities are required. A multi-role phased array antenna needs to be capable of broad-band and/or wide-scan capabilities to fit tasks such as radar, data links and electronic warfare.

An antenna element that is promising for multi-role phased array antennas is the fragmented aperture element. This antenna element consists of a conducting pattern etched on a dielectric substrate backed by a groundplane. The conducting pattern, dielectric thickness and permittivity are designed with the help of a genetic algorithm (GA). The cost function is evaluated using a finite-difference time-domain (FDTD) code with periodic boundary conditions [1].

One of the first studies on fragmented aperture arrays was presented in [2]. However, no results were given for groundplane backed arrays scanned off broadside. Later, Thors et al. [3-4] studied fragmented aperture arrays with focus on broad-band properties when scanning 45° ($SWR \leq 2$ E plane and H plane). In [3-4] each pixel was represented by a single FDTD-cell. It was shown that using a single FDTD-cell for each pixel agreed well with higher resolution meshes for broadside scan. However, when the array was scanned in the E plane and H plane, respectively, the performance decreased [5]. Hence, the bandwidth requirement was no longer met.

The focus of this paper is to study some of the practical problems that need to be solved before manufacturing these array elements. Furthermore, the wide-scan properties are discussed by increasing the scan range up to 60°.

One possible problem for these elements is that electrical contacts between corners of diagonally adjoining pixels in the aperture are difficult to manufacture. To avoid manufacturing problems two strategies are investigated to avoid connection problems. Another problem that needs to be investigated is the choice of materials. In [3-4] the dielectric constant of the substrate was a parameter that could change linearly; this resulted in materials that were not commercially available. The simulations will now be restricted to a list of commercially available dielectrics. Finally two designs are presented of thin fragmented aperture elements for scan angles out to 60° from broadside.

2. ARRAY ELEMENT

The antenna is a large planar phased array with the antenna elements placed in a quadratic grid. The antenna is assumed to be sufficiently large so that it can be approximated by an infinite periodic antenna. This allows a unit-cell description of the array.

The antenna element consists of a fragmented metallic pattern on a substrate backed by a ground plane. On top of the element one or several layers of superstrates can be added, in this paper one or no layer is used. The metallic pattern consists of 20x20 metallic pixels. The element is fed with a discreet source in the middle of the unit-cell, see Fig. 1. The metallic pattern is symmetric and can be described by a quadrant of the element. In a 10x10 pixel quadrant 8 pixels are fixed so that the geometry around the source is fixed. The remaining pixels, dielectric constants, and dielectric sheet thicknesses are determined by

Proc. 'EuCAP 2006', Nice, France
6–10 November 2006 (ESA SP-626, October 2006)
Authorized licensed use limited to: JAMES MALONEY. Downloaded on February 18,2026 at 12:06:39 UTC from IEEE Xplore. Restrictions apply.

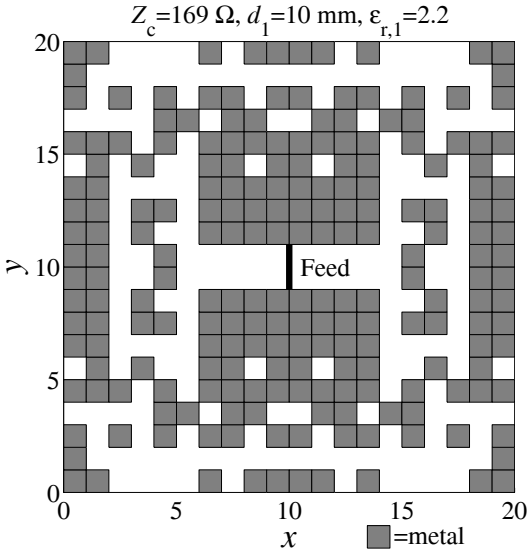

Figure 1. A typical unit cell geometry for a fragmented aperture antenna

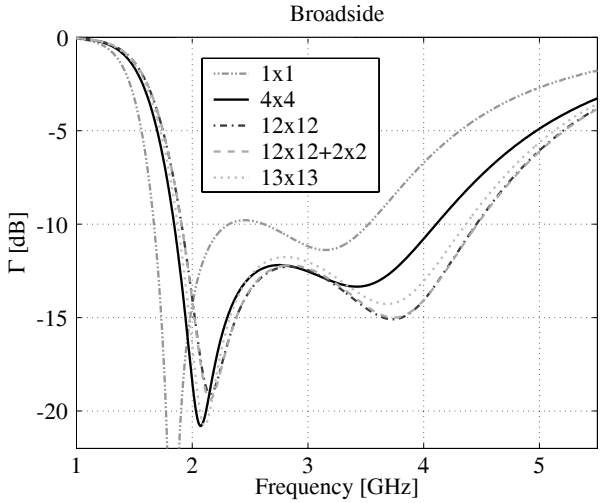

Figure 2. Results for broadside scan for the unit cell geometry shown in Fig. 1 for different mesh solutions and critical corner solutions.

a GA. In the numerical calculations the GA is used to minimize a fitness function. The fitness function is given as a sum of the reflected energy for three scan directions over a certain frequency range. Hence, the fitness function is given as

$$F = \sum_i \sum_j w_{ij} \left|\Gamma(\Omega_i, f_j)\right|^2 \tag{1}$$

where Γ is the reflection coefficient, f_j denotes the discrete sample frequencies over the design band, Ω_i denotes the different scan directions and w_{ij} is a weight function. The weight function,

$$w_{ij} = \sin(\pi \frac{f_j - f_{\text{low}}}{f_{\text{high}} - f_{\text{low}}}) \tag{2}$$

defines a center frequency in the frequency band of operation, and f_{high} and f_{low} are constants which have values higher and lower than that of the design band.

An often used characteristic impedance is $50\ \Omega$, but this may not be the ideal impedance in the broad-band or wide-scan perspective. Therefore, the characteristic impedance of the feed point is allowed to take values between $20 - 300\ \Omega$. The fitness function (Eq. 1) is calculated for these impedances and the best is chosen. Thus, the characteristic impedance is not a part of the chromosome, and do not increase the number of unknowns in the GA.

The reflection coefficient is computed with FDTD with periodic boundary conditions [1]. Earlier work [3] used one FDTD-cell to describe each pixel in the element. This was sufficient for broadside-scan but was not enough when the array was scanned to 45° from broadside. After some analysis using different resolutions in the FDTD-mesh it was found that using 4x4 FDTD-cells per pixel agrees well with higher resolution meshes, both for broadside and large scan angles (see Fig. 2-4 for a typical example). Therefore 4x4 FDTD-cells were used to describe each pixel in the optimization. This, of course, increased the simulation time considerably. An optimization of one antenna element now takes several weeks on an Intel Pentium 4, 2 GHz system, compared to days with the 1x1 FDTD-cell per pixel mesh.

3. CORNER TO CORNER CONTACT

The electric contact between pixels that are adjoint diagonally to each other is a problem that needs to be addressed before manufacturing an antenna, see Fig. 5a. The diagonally positioned pixels have an infinitely small contact point. This is difficult to manufacture and ohmic effects may also be a problem. To avoid this type of contact pixels can be removed or added manually at these critical points. The GA could also remove geometries that have this configuration of pixels, but they are very frequent and it is better if a method that simplifies the manufacturing process is used. To study this the geometry shown in Fig. 1 is used. It is an element without a superstrate and the thickness of the substrate is $d_1 = 10$ mm and $\varepsilon_{\text{r},1} = 2.2$.

One way of dealing with a critical diagonal pixel contact is to add a smaller pixel over the critical corner, as illustrated in Fig. 5b. Calculations were made using 12x12 FDTD-cells per pixel, and compared with calculations using 12x12 FDTD-cells per pixel plus an extra 2x2 FDTD-cell pixel positioned over each critical corner. The difference in the results are negligible as can be seen

Authorized licensed use limited to: JAMES MALONEY. Downloaded on February 18,2026 at 12:06:39 UTC from IEEE Xplore. Restrictions apply.

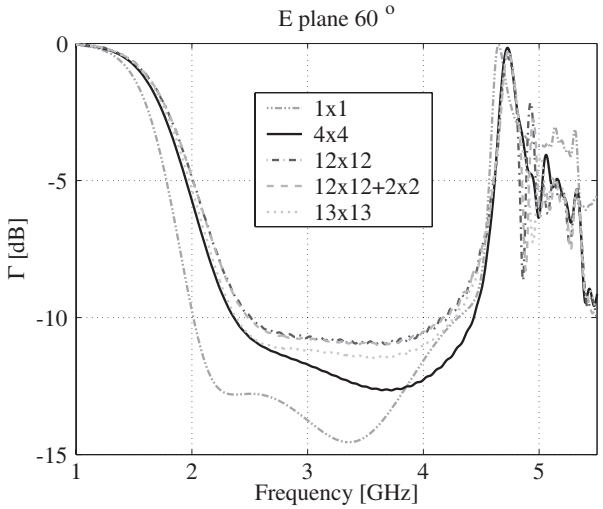

Figure 3. Results for scan out to $60°$ *from broadside in the E plane (zy plane) for the unit cell geometry shown in Fig. 1 for different mesh solutions and critical corner solutions.*

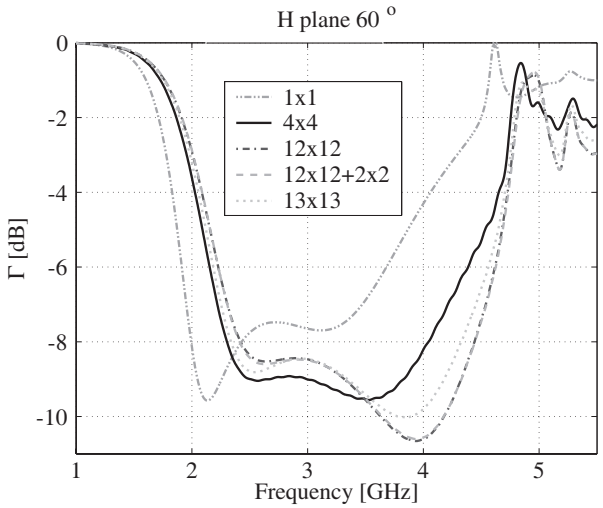

Figure 4. Results for scan out to $60°$ *from broadside in the H plane (zx plane) for the unit cell geometry shown in Fig. 1 for different mesh solutions and critical corner solutions.*

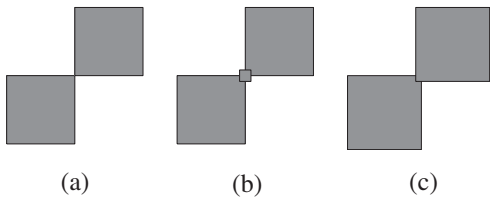

Figure 5. (a) Showing a critical diagonal pixel contact. (b) Shows the small patch covering the critical corner to ensure electrical contact. (c) Shows how overlaping pixels are used to ensure electrical contact.

in Fig. 2-4. This shows that the critical corner contact can easily be avoided by adding additional metal to ensure electrical contact.

Another way to solve this problem is to increase the size of the pixels so that the pixels have a small overlap, Fig. 5c. This may seem to be a larger step from the original pattern with 4x4 FDTD-cells per pixel than the pattern with added pixels but this is not correct. The results when using 13x13 cells per FDTD-cell with one overlapping FDTD-cell agrees better with the results from the 4x4 mesh than the 12x12 pattern. This is because the physical width of a cell in FDTD is slightly larger than the numerical width. The problem is that FDTD do not handle field singularities correct. These effects can be corrected as explained in [6], but these modifications are not included in the code used here. However, it is shown in [6] that the physical size of an edge is extended 0.19Δ where Δ is the FDTD-cell width. Experience from modeling striplines shows that a value of 0.25Δ produces a better result [7]. If this value is used for the extension of the physical width of the pixels, the physical pixel will become 0.5Δ wider than in the mesh. According to this rule of thumb, a pixel with a width of 13 FDTD-cells and $\Delta = 0.125$ mm have the same physical width as a pixel with a width of 4 FDTD-cells and $\Delta = 0.375$ mm. Therefore the overlapping pixel is a better description of the optimized pattern than the 12x12 FDTD-cell mesh.

4. THIN ELEMENT DESIGN

In previous designs no consideration was taken to the available dielectric materials that were used in the optimization. This led to designs that were difficult to manufacture, and changing ε_{r} to commercially available materials changed the performance too much. Therefore, a new effort is made to design an element where only four materials are allowed $\varepsilon_{\mathrm{r}} = 1.1, 2.2, 3.0$, and 3.38.

The antenna elements are placed in a quadratic grid with an element spacing of 30 mm. The thickness of the substrate d_1 is allowed to vary from $5.33 - 10$ mm, and have the dielectric constant $\varepsilon_{\mathrm{r},1}$. If a superstrate is included its thickness d_2 varies between $0.66 - 8$ mm, and the dielectric constant is denoted $\varepsilon_{\mathrm{r},2}$. The design band is $1.5 \leq f_i \leq 4.5$ GHz, and the fitness function constants are $f_{\mathrm{low}} = 0.8$ and GHz $f_{\mathrm{high}} = 5.5$.

Three scan directions are used when calculating the fitness-function, broadside, E plane $60°$ and H plane $60°$. For smaller angles the reflection coefficient are in general better than for the large angles and to reduce the optimization time these are omitted when calculating the fitness function. In the results the bandwidth $BW_{SWR \leq X}$ is defined as the ratio between the highest and lowest frequency for which $SWR \leq X$ for all scan directions, where SWR is the standing wave ratio. Two additional scan directions, E plane $45°$ and H plane $45°$, are calculated after the optimization and are also shown in the results for the elements.

Authorized licensed use limited to: JAMES MALONEY. Downloaded on February 18,2026 at 12:06:39 UTC from IEEE Xplore. Restrictions apply.

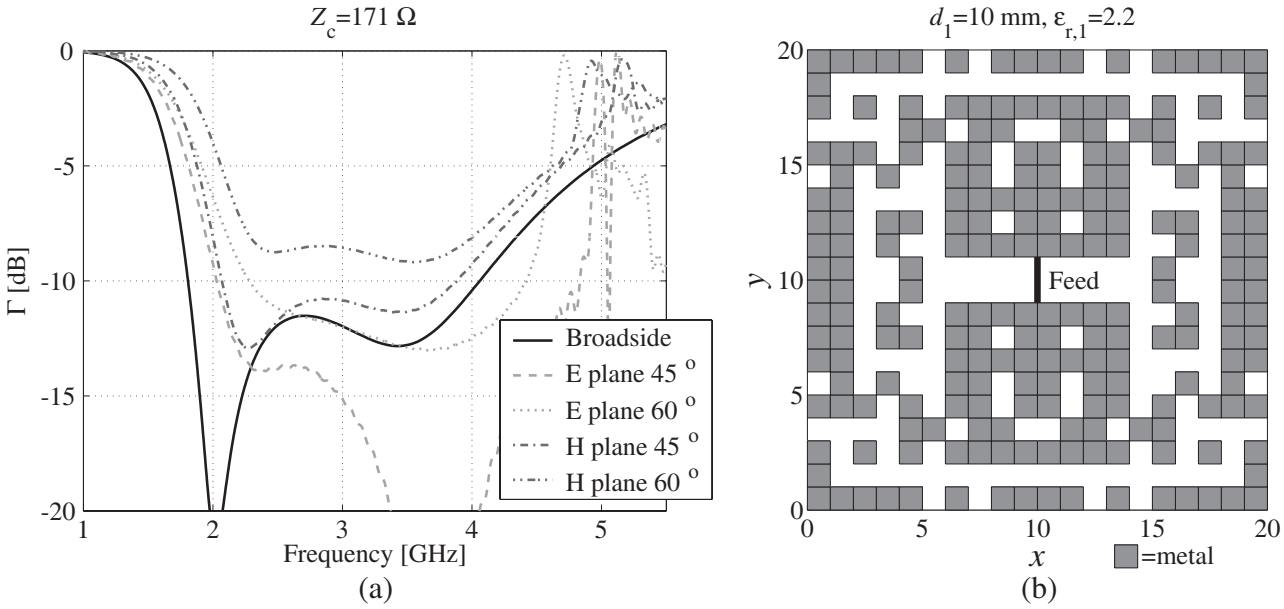

Figure 6. Design results for array antenna without superstrate. (a) Reflection coefficient. (b) Unit-cell geometry.

4.1. Element without a superstrate

For the element shown here $d_1 = 10$ mm and $\varepsilon_{\mathrm{r},1} = 2.2$ with the characteristic impedance $Z_c = 171\ \Omega$. The element performs best in the E plane and have problems in the H plane, as seen in Fig. 6. Hence, the H-plane performance limits the bandwidth. For scan out to $60°$ from broadside there is no frequency band for which the element fulfills the design goal SWR≤ 2. However, for SWR≤ 3 ($\Gamma = -6$ dB) the bandwidth is $BW_{SWR\leq 3} = 2.07$.
For scan out to $45°$ in all planes the bandwidth is $BW_{SWR\leq 2} = 1.94$. The H-plane performance is still the limiting band. The thickness of the element is the maximum allowed by the GA and a performance increase is easiest to achieve by allowing the element to become thicker.

4.2. Element with a superstrate

Next, we allowed the GA to include a superstrate. The element has a substrate with thickness $d_1 = 8.67$ mm and $\varepsilon_{\mathrm{r},1} = 3.00$. The GA choose the maximum thickness of the superstrate $d_2 = 8.00$ mm and $\varepsilon_{\mathrm{r},2} = 3.38$. The characteristic impedance for this element is $Z_c = 173\ \Omega$.

Adding one or several layers of dielectric superstrates above the fragmented patch was shown in [4] to improve bandwidth. This is also the case now, Fig. 7. The H-plane bandwidth have improved for scan out to $45°$ in all planes with a bandwidth $BW_{SWR\leq 2} = 2.20$. For scanning out to $60°$ in all planes $BW_{SWR\leq 3} = 2.16$. However, the match of the element is generally poorer for the E plane and H plane. The local maxima for Γ within the design band are higher for the element with a superstrate than for the one without. The superstrate also introduces a surface wave around 4 GHz.

5. CONCLUSIONS

A phased array antenna has been described in this paper that was designed with the help of a GA for scan angles out to $60°$ from broadside. The focus has been on simplifying the manufacturing of the diagonally adjoining pixels and numerical results for thin antennas.

The best solution to the corner to corner contact is overlapping pixels, since this method is easy to manufacture but it is also a good description of a sparse mesh in FDTD.

Two antenna elements were synthesized with the genetic algorithm. Both elements had a bandwidth of around $BW_{SWR\leq 2} = 2$ for scan angles out to $45°$ form broadside and $BW_{SWR\leq 3} = 2$ for scan angles out to $60°$ in all planes. The synthesized elements have taken the maximum allowed thickness and it is most likely that the performance can be improved by allowing the elements to be thicker, especially the substrate thickness. Allowing the superstrate to become thicker could introduce resonances and surface waves for lower frequencies within the design band. The fitness function used have a problem eliminating such solutions and needs to be modified to avoid them. Another problem with the fitness function is that it sometimes favor the broadside performance at the cost of the scanned angles. To solve this the weight of the large scan angles needs to be increased or more scan directions are needed.

Authorized licensed use limited to: JAMES MALONEY. Downloaded on February 18,2026 at 12:06:39 UTC from IEEE Xplore. Restrictions apply.

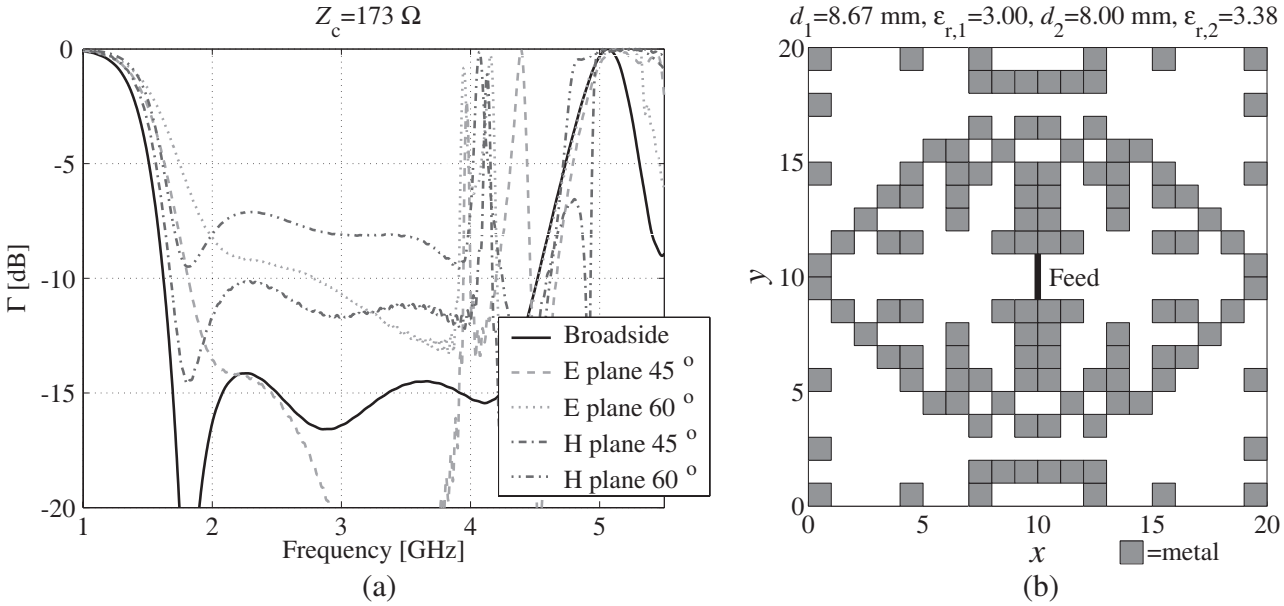

Figure 7. Design results for array antenna with a superstrate. (a) Reflection coefficient. (b) Unit-cell geometry.

ACKNOWLEDGMENTS

The contribution of Dr. Henrik Holter who provided the PB-FDTD code and basic GA-code, is gratefully acknowledged.

REFERENCES

[1] Holter H. and Steyskal H., "Infinite phased-array analysis using FDTD periodic boundary conditions-pulse scanning in oblique directions," *IEEE Antennas and Propag.*, vol. 47, no. 10, pp. 1508-1514, Oct. 1999.

[2] Friedrich P., Pringle L., Fountain L., Harms P., Smith G., Maloney J., and Kesler M., "A new class of broadband planar apertures," *Antenna Application Symposium,* Allerton Park, IL, Nov. 2001, pp. 561-587

[3] Thors B., Steyskal H. and Holter H., "Broad-band fragmented aperture phased array element design using genetic algorithms," *IEEE Antennas and Propag.*, vol. 53, no. 10, pp. 3280-3287, Oct. 2005.

[4] Thors B. and Steyskal H., "Synthesis of broadband fragmented aperture array elements using algorithms," *Alfvén Lab., Royal Inst. of Technology, Stockholm*, Sweden, Tech. Rep. TRITA-TET 2004:3, 2004.

[5] Steyskal H. and Holter H., Private communication, 2006.

[6] Shorthouse D. B. and Railton C. J., "The incorporation of static field solutions into the finite-difference time domain algorithm," *IEEE Trans. Microwave Theory Tech.*, vol. 40, no 5, pp. 986-994, May. 1992.

[7] Holter H., "Handbook PB-FDTD ver. 3.3," Stockholm, Sweden, 2006.

Authorized licensed use limited to: JAMES MALONEY. Downloaded on February 18,2026 at 12:06:39 UTC from IEEE Xplore. Restrictions apply.